Applied Energy 88 (2011) 3726–3736

Contents lists available at ScienceDirect

Applied Energy

journal homepage: www.elsevier.com/locate/apenergy

Optimized solar-powered liquid desiccant system to supply building fresh water and cooling needs

N. Audah, N. Ghaddar *, K. Ghali

Department of Mechanical Engineering, American University of Beirut, P.O. Box 11-0236, Beirut 1107 2020, Lebanon

ARTICLE INFO

Article history:
Received 25 November 2010
Received in revised form 6 April 2011
Accepted 10 April 2011
Available online 4 May 2011

Keywords:
Solar-powered liquid desiccant system
Water extraction from atmosphere
Design optimization of liquid desiccant system
Dehumidification/humidification processes

ABSTRACT

This paper studies the feasibility of using a solar-powered liquid desiccant system to meet both building cooling and fresh water needs in Beirut humid climate using parabolic solar concentrators as a heat source for regenerating the liquid desiccant. The water condensate is captured from the air leaving the regenerator. An integrated model of solar-powered calcium chloride liquid desiccant system for air dehumidification/humidification is developed. The *LDS* model predicted the amount of condensate obtained from the humid air leaving the regenerator bed when directed through a coil submerged in cold sea water. An optimization problem is formulated for selection and operation of a *LDS* to meet fresh water requirement and air conditioning load at minimal energy cost for a typical residential space in the Lebanon coastal climate with conditioned area of 80 m^2 with the objective of producing 15 l of fresh drinking water a day and meet air conditioning need of residence at minimum energy cost. The optimal regeneration temperature increases with decreased heat sink temperature with values of 50.5 °C and 52 °C corresponding to sink temperatures of 19 °C and 16 °C.

1. Introduction

The continuing rise in energy demand and costs and the associated environmental problems, notably climate change, is causing increased emphasis in finding more efficient ways to condition our closed spaces without having to harm our environment. In the hot and humid climates of the Middle East, where clean fresh water is a scarce resource, and a comforting surrounding is not naturally available we have two major needs of occupants. These include the need to dehumidify air that meet comfort conditions while at the same time have a fresh water supply. Atmosphere is a large reservoir of water in humid climates. Producing water from the atmosphere in humid areas may become the least damaging method to environment. Increased brine reject from the multiple water desalination plants on the Gulf shore has increased salt concentration to levels impacting marine flora in the Gulf water. Soil deterioration influenced by land disposal of brine from water desalination plants is already reported by Al-Faifi et al. [1] at several locations of desalination plants at Saudi Arabia. Both fresh water and air conditioning needs can be met by a hybrid system that combines both functions of dehumidification/humidification of atmospheric air in one unit to effectively meet these two requirements at low impact on the environment and reduced energy cost. This can be done through the use of the growing technology of liquid desiccant solutions (calcium chloride in our case) running through a dehumidifier/regenerator system. On the one hand these special types of chemicals which enter the dehumidifier give us the ability to remove excess water vapor from the air which can be used as fresh water and on the other hand it would provide a stream of dry air at temperatures that can be supplied to the building for air conditioning.

Researchers have developed solar powered air conditioners to meet the air conditioning needs using desiccant dehumidification or absorption chillers [2–6]. However, meeting both air conditioning and water needs in one solar-powered desiccant system has not been addressed. The developing field of aqueous desiccant dehumidification looks to be an attractive solution which helps us combine all of our requirements of having conditioned air, fresh water supply, and an environmentally safe alternative operating system all in one. Fumo and Goswami [7] investigated the effect of various input conditions to the dehumidifier as well as regenerator and how it affects their operation. Afandizadeh and Foumeny [8] studied two major types of dehumidification beds; random packed and structured packed beds and reported the influence of the type of pores and their geometry in pressure drops across beds. Al-Farayedhi et al. [9] and Al-Sulaiman et al. [10] focused on obtaining correlations which help analyze the dehumidification of any dehumidifier regardless of the type of desiccant we are using, as long as it is an aqueous liquid type. Al-Sulaiman et al. [10] analyzed the influence of varying desiccant flow rate in increasing the condensation of water vapor. Elsarrag [11] reported

* Corresponding author. Tel.: +961 1 350000 2513; fax: +961 1 744462.
E-mail address: farah@aub.edu.lb (N. Ghaddar).

0306-2619/$ - see front matter © 2011 Elsevier Ltd. All rights reserved.
doi:10.1016/j.apenergy.2011.04.028

Nomenclature

A	area, m^2
A_a	aperture area of the collector, m^2
A_r	receiver area of the concentrator, m^2
A_s	interfacial area for absorption with an aqueous solution, m^2/m^3
C_{pa}	specific heat of air, J/kg K
C_{pw}	specific heat of liquid desiccant, J/kg K
C_{pv}	specific heat of water, J/kg K
eff	effectiveness, efficiency
F_R	collector heat removal factor
G	mass flow rate per unit cross-sectional area of bed, kg/m^2 s
h	heat transfer coefficient, W/m^2 K
h_D	mass transfer coefficient, m/s
h_{fg}	heat of condensation of water, J/kg
i	discount rate (%)
$I_{E,HST}$	hourly energy consumption at given heat sink temperature, W/h
I_{HST}	total cost function for a given heat sink temperature, $
$I_{i,HST}$	capital initial cost associated with the number of solar concentrators, $
$I_{op,HST}$	total operational cost over the equipment operational life cycle cost over n years
L	length of bed (m)
LCC	investment life cycle cost, year
LDS	liquid desiccant system
$\dot{m}$	mass flow rate, kg/s
n	number of years
q	ratio of regenerator to dehumidifier air flow rates
q_b	binding energy between desiccant and water, J/kg
Q_R	rate of regeneration heat, W
Q_u	useful energy from collector, W
r	mass ratio of the desiccant flow rate to the dehumidifier air flow rate
S	absorbed radiation by collector, W/m^2
T	temperature, °C
T_{aid}	air temperature at inlet to dehumidifier, °C
T_{lid}	liquid temperature at inlet to dehumidifier, °C
$T_{li,sh}$	liquid desiccant temperature at inlet to the solar heater, °C
T_{lod}	liquid temperature at outlet of dehumidifier, °C
T_{lohe}	liquid temperature at outlet of heat exchanger and entering the solar heater, °C
T_{lor}	liquid temperature at outlet of regenerator, °C
$T_{lo,sh}$	liquid desiccant temperature at outlet of the solar concentrator system, °C
T_{ref}	reference temperature for enthalpy, °C
T_{reg}	regeneration temperature, °C
U_L	overall heat transfer coefficient, W/m^2 K
$(UA)_t$	tank overall heat loss factor, W/°C
V	volume in m^3
W	specific humidity ratio, kg_w/kg_a
W_l^*	specific humidity of air in equilibrium with solution, kg_w/kg_a
x	distance from the bottom of bed, m
Y	moisture content of solution (mass of water/desiccant)
Y_{lid}	moisture content at inlet to dehumidifier
Y_{lod}	moisture content at outlet of dehumidifier

Greek

ρ	density, kg/m^3

Subscripts

a	air
l	liquid desiccant
s	storage tank
sh	solar heater

the influence of varying air flow rate, inlet desiccant temperature, as well as desiccant concentration and inlet air humidity on the condensation rate. His work showed that as the inlet desiccant temperature increases the evaporation rate increases, i.e. condensation rate decreases. Moreover as inlet desiccant concentration increases evaporation decreases and as air humidity ratio increases, a drop in evaporation rate is experienced. In addition, he reported that the optimum liquid to air mass flow rate ratio is 2.54 [11]. Other work developed by Ghaddar et al. [12] is based on dehumidifier simulation model which uses mass and energy balance equations. They examined the economical feasibility of applying a hybrid system to reduce operational energy required, and the benefit of downsizing an AC system.

According to Gandhidasan [13], for temperatures as low as 20 °C of the strong liquid desiccant, the temperature of the dry air stream leaving dehumidifier is higher than the typical supply air temperature room summer comfort conditions of 23–25 °C. If a liquid desiccant system is to provide the entire cooling needs of indoor space at high room temperature, other means for attaining thermal comfort conditions, such as enhanced air motion in the space, are needed. Messaoudene et al. [14] reported that the indoor air motion can go up to 1 m/s and to 1.5 m/s using ceiling fans without causing thermal discomfort (draft) with room air temperature ranging from 29 °C to 34 °C. They considered the effect of ceiling fan ventilation on thermal comfort and concluded that simple air motion can lead to an acceptable thermal comfort sensation improvement under warm conditions particularly in the case when occupants are allowed to select air speed on their own. Liping and Hien [15] demonstrated by experiments that it is possible to maintain comfortable conditions up to 31 °C (1.0 met) and 29 °C (1.2 met) if an air speed of 1 m/s or greater is available over the upper body. Arens et al. [16] indicated that thermal comfort conditions with the space can be attained when the air temperature and relative humidity do not exceed of 32 °C and 40% RH, respectively.

It is of interest to know if the two needs of fresh water and air conditioning can be met by the *LDS* while entirely powered by solar energy in Beirut humid climate. This paper will focus on the feasibility of using a solar-powered liquid desiccant system to meet both needs at minimum cost. Parabolic solar concentrators will be the heat source for regenerating the liquid desiccant. The water condensate will be captured from the air leaving the regenerator. The design variables will be identified and the *LDS* design will be optimized based on optimizing initial and operative cost. Models will be developed for the components of the *LDS* comprised of solar humidifier, desiccant dehumidification and cooling plant and will be used in the design and optimization process. A case study is presented to assess the integrated system performance in achieving the dual function of delivering water and comfort for Lebanon's climate.

2. System description and problem statement

Fig. 1 depicts the solar-powered liquid desiccant system (*LDS*) and condensing unit. The system is composed of a dehumidifier, regenerator, parabolic solar collectors, heat exchangers, and

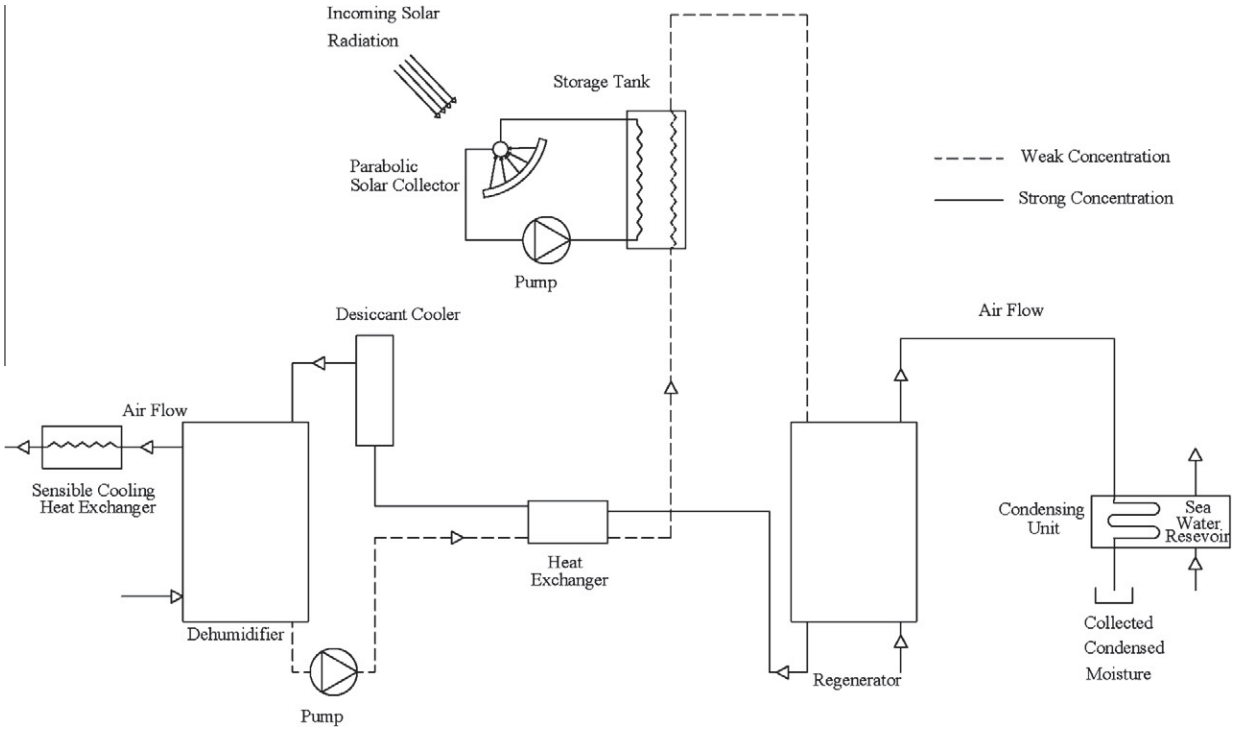

Fig. 1. Schematic of the liquid desiccant system.

desiccant cooler. The input variables of the dehumidifier are the ambient air temperature and humidity ratio, the flow rate of the desiccant calcium chloride solution and the air flow rate. The entering humid air moisture is absorbed by the desiccant. The air leaving the desiccant bed is used for household air conditioning. The liquid desiccant leaving the dehumidifier enters a heat exchanger where it is warmed up. It is further heated before entering the regenerator by another exchanger in the water storage tank heated indirectly by solar energy transmitted from the concentrators' closed fluid circuit. The hot low concentration liquid desiccant enters the regenerator where counter flow ambient air absorbs the water accumulated from the desiccant. The regenerator exit humidified air is directed to a cooling coil submerged in cold sea water (temperature varying between 16 °C and 20 °C depending on depth from which it is withdrawn) where condensation occurs and distilled water is collected. Several researchers have concluded that the separation of the evaporation and condensing parts of the solar still into two distinct parts will lead to a reduction in thermal inefficiencies and improved overall performance [17–22]. This separation into evaporation (humidification) and condensation (dehumidification) components is the underlying principle for the humidification–dehumidification technology which is currently receiving a great deal of attention in the literature as it may yet prove to be the technology of choice for inexpensive decentralized small scale desalination plants. The desiccant that leaves the regenerator re-enters the dehumidifier after it is cooled down and the loop is closed.

The sizing and operation of the integrated system components observes the following conditions/constraints:

- The best practice ratio r of desiccant flow rate G_l to air flow rate G_a is 2.54 as reported by Elsarrag for calcium chloride [11]. It can vary from 1 to 5.
- The moisture content of the desiccant solution at inlet to the dehumidifier is set to a maximum value of $Y = 1.5$ to avoid the problem of crystallization of $CaCl_2$ [12], where Y is the ratio of the mass of water to the mass of the desiccant and corresponds to a desiccant concentration of 40% by weight. The calcium chloride is a weak desiccant compared to other hygroscopic salts such as lithium bromide but is selected because of its safety characteristics.
- The lowest temperature permitted of the desiccant entering the regenerator should be above 50°C for effective regeneration of the desiccant.
- Temperature of the desiccant entering the dehumidifier depends on heat sink and its maximum value is set at 30 °C.
- The number of hours of operation of the system is assumed nine hours per day to produce the needed amount of water and provide the air conditioning needs.
- Concentrators and storage tank are of sufficient size to provide heat input needs of the regenerator. The solar concentrator system would occupy smaller roof area and sustain longer hours of high grade energy when compared with roof area needed and operational hours of flat plat collector system to deliver same heat input [12].
- The heat sink is taken as a typical sea bed with 20 °C and it can get as low as 16 °C.

The remaining operational variables to the design are the ambient air humidity and air temperature (not under our control) and the appropriate air and desiccant flow rates to meet needs.

To be able to size and model the system operation to meet desired requirements, the modeling of flow and thermal variables will be normalized per unit area of the dehumidifier. The maximum flow of air going into the dehumidifier is the key parameter for the design since it is directly correlated to desired water output and dry air stream conditions supplied to the space. For the solar parabolic concentrator sizing, one solar module specification is adopted and based on the demand, we determine how many solar modules are needed to meet heating requirements for air and liquid desiccant entering the regenerator. To design the *LDS* for the identified water and air conditioning needs, the dehumidified supply air should provide comfort to the space during the 9-h

operation period including the peak load hour and the total amount of collected water over the 9-h operation is equal to the identified value. The maximum dehumidifier air flow rate should be equal to that design value determined at peak load. The design variables for the integrated system are interdependent as follows:

1. The mass flow rates of the air in the regenerator and in the dehumidifier. The value of this air flow rate is dictated by the most critical output need (air conditioning/fresh water) throughout the cooling season for Beirut climate.
2. The temperature of regeneration which affects the amount of absorbed water and the dryness of the dehumidifier exit air stream.
3. The heat sink temperature which if decreased increases the potential of increasing the range of heat regeneration resulting in better water production, and decreased air flow rate.

The main design parameters of the packed beds that will be sized are: (a) The flow rate ratio "r" of the mass flow rate of $CaCl_2$ liquid "G_l" to the mass flow rate of air "G_a" in the dehumidifier; and (b) the ratio "q" of total air flow rate in the regenerator to that in the dehumidifier is taken as 1.0 in this work [12]. Inlet conditions of both air and liquid desiccant to the dehumidifier are governed by ambient dry bulb and wet bulb temperatures. The temperature of air at inlet to the dehumidifier T_{aid} and its specific humidity w_{aid} depend on conditions of the outdoor air. The concentration of the desiccant solution at inlet to the dehumidifier is set to 0.4.

3. *LDS* design and operation optimization problem

To design the *LDS* for identified water and air conditioning needs, we have to calculate the space peak load conditions and identify the peak load design values for air supply temperature, humidity ratio and air flow rate. The maximum dehumidifier air flow rate should be equal to that design value. Since we have more than one desired objective for the system outputs, an optimized design is sought such that the overall system incremental capital cost and the operational cost in the cooling season over the system life cycle is minimized. The regeneration temperature affects the amount of absorbed water and the dryness of the dehumidifier exit air stream.

The needed air flow rate for meeting the two objectives of the system is lower for higher regeneration temperature which leads to lower operational LDS fans' cost while increasing the capital cost due to the need of higher number of parabolic concentrators. A lower heat sink temperature increases the potential of increasing the heat regeneration resulting in better water production, and decreased air flow rate (i.e. lower operational cost). On the downside this will require additional number of solar collectors.

The independent design input variable is the heat sink temperature which determines the number of solar concentrator modules and the size of the fans. The number of solar modules affects the first cost, while the fans' sizes affect the operational cost. The optimal design and operation of the system will be based on the investment life cycle cost of the *LDS* including capital cost invested in the number of the solar concentrators and the cost of the system operation over 20 years. In this study, an initial extra expenditure is invested at a market discount rate $i = 0.03$, in order to make a saving in the yearly energy bill over a period $n = 20$ years. The optimization of the *LDS* cost (incremental depending on added number of solar modules and operational) of the solar-powered *LDS* requires the minimization of the following function over 20 year of operation:

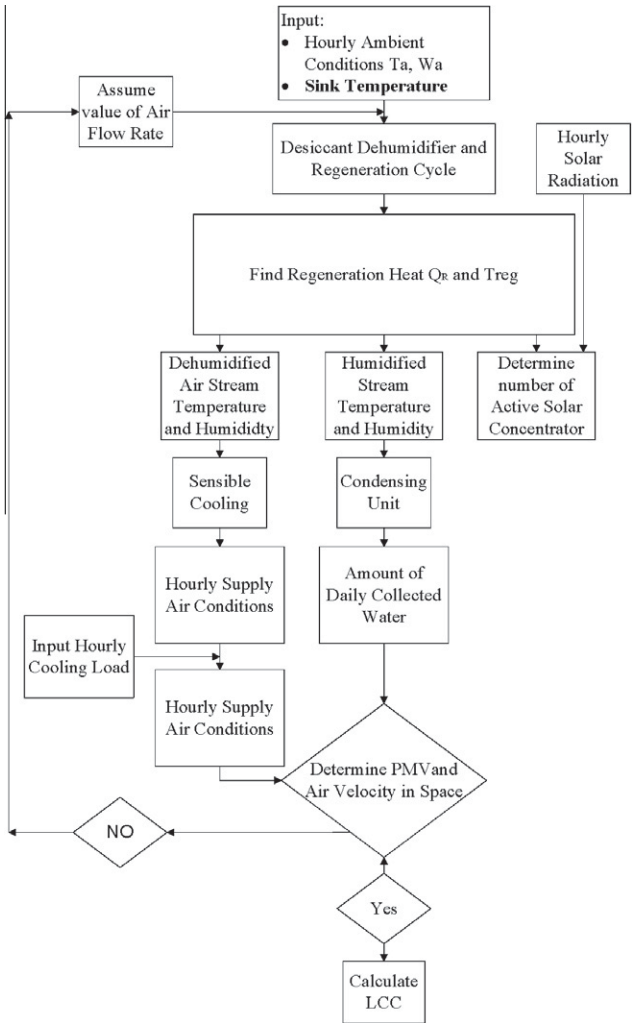

Fig. 2. Flow chart of the solution and optimization procedure.

$$I_{HST} = I_{i,HST} + I_{op,HST}$$

where

$$I_{op,HST} = \frac{(1+i)^n - 1}{i(1+i)^n} \times \left(\sum_{\text{June}}^{\text{Sep}} \sum_{i=1}^{\text{days in month}} \sum_{9:00\ \text{AM}}^{6:00\ \text{PM}} I_{E,HST} \right) \times \underbrace{\frac{\$}{\text{KW h}}}_{\text{conversion}} \quad (1)$$

where I_{HST} is the total cost for a given heat sink temperature, $I_{i,HST}$ is the capital initial cost associated with the number of solar concentrators, $I_{op,HST}$ is the total operational cost over the equipment operational life of n years using interest rate i, and $I_{E,HST}$ is the hourly energy consumption by the two fans and the liquid desiccant circulation pump. The energy cost associated with the pump and the internal circulation fan in the residential space is not included in the operation cost since their energy use will be negligible compared to the cost of the fans of the desiccant towers.

The heat sink ranges from 16.0 °C to 20.0 °C based on sea water conditions for the cooling exchanger. The sink temperature is a critical optimization parameter since the concentration of the liquid desiccant calcium chloride is not a variable and has already been fixed at 0.4 to avoid crystallization. If the sink temperature is decreased then regeneration temperature increases and hence increasing the number of solar concentrators and the incremental initial cost. Decreasing the flow rate of air and desiccant streams means we have lower operating cost which means that optimum values exist for regeneration temperature, air flow rate, and number of solar concentrators.

The optimal operational parameters of air flow rate for given sink temperature is selected based on simple search method after multiple simulations of the system operation for multiple designs performed at different airflow rates. The total number of simulations performed exceeded 100 for ranges of regeneration temperatures between 51 °C and 58 °C for several sink temperatures between 16 °C and 20 °C. The optimal regeneration temperature for a given heat sink temperature will be found based on finding the investment life cycle cost *LCC* based on the saving in cost compared to the cost of the base case at sink temperature of 20 °C as follows:

$$LCC = \frac{I_{i,HST} - I_{i,20\ ^\circ C}}{(I_{op,20\ ^\circ C} - I_{op,HST})/n} \tag{2}$$

It is clear that the sizing of the complete system requires development and use of simulation models of the performance of each component of the system. Standard mass and energy balances over each component of the desiccant system and heat exchangers will be performed in accordance to component models as will be described in the next section. Fig. 2 presents a flow chart of the proposed optimization procedure.

4. Mathematical formulation of system component models

4.1. Model equations of dehumidifier and regenerator

The process of air dehumidification or liquid desiccant regeneration in the packed beds of the dehumidifier and the regenerator is done using mathematical models of Radhwan et al. [22] and Ghaddar et al. [12] where standard mass and energy of air and liquid desiccant are formulated using 1-D flow models in the packed beds and assuming quazi-steady state processes, uniform properties for both air and liquid desiccant over the working range, and constant heat and mass transfer coefficients; The mass conservation of water vapor in air and liquid desiccant streams are given respectively by

$$\frac{dW}{dx} = \frac{\rho_a h_D A_s}{G_a}(W_l^* - W) \tag{3a}$$

$$\frac{dY}{dx} = \frac{\rho_a h_D A_s}{G_l}(W_l^* - W) \tag{3b}$$

The energy balances for the air and liquid desiccant stream are respectively given by

$$(C_{pa} + WC_{pv})\frac{dT_a}{dx} + C_{pv}\frac{dW}{dx}(T_a - T_{ref}) + \frac{hA_s}{G_a}(T_a - T_l) = 0 \tag{4a}$$

$$(C_{pl} + YC_{pw})\frac{dT_l}{dx} + C_{pw}\frac{dY}{dx}(T_l - T_{ref}) + \frac{dY}{dx}q_b = \frac{\rho_a h_D A_s}{G_l}(W_l^{ast} - W)h_{fg} - \frac{hA_s}{G_l}(T_a - T_l) \tag{4b}$$

where T_a and T_l are the air and desiccant temperatures, respectively. The mass and energy balances are subject to the following boundary conditions:

$$\text{At the bottom } x = 0: \quad W = W_{aid}, \quad T_a = T_{aid} \tag{5a}$$

$$\text{At the top } x = L: \quad Y = Y_{lid}, \quad T_l = T_{lid} \tag{5b}$$

where W_{aid} and T_{aid} are the specific humidity and the temperature of the air at inlet to the dehumidifier, and Y_{lid} and T_{lid} are the moisture content and the temperature of the liquid at inlet to the dehumidifier. Similar boundary conditions are used when formulating the flow in the regeneration bed. The mass and heat transfer coefficients use values published by Ertas et al. [23] and are the same values used in the work Radhwan et al. [22].

The dehumidification and regeneration processes' model solution is performed using a fourth order Runge–Kutta scheme to integrate the moisture and energy balances of air and liquid desiccant in the packed beds during the air dehumidification mode and the solution generation mode. For known inlet conditions of air and liquid desiccant, the numerical model calculates the air and liquid desiccant temperatures, the air humidity ratio, and the liquid desiccant moisture content in the packed beds at various bed heights as well as exit conditions of the liquid desiccant and air and solution flow rates. The liquid desiccant process models were validated by reproducing the published results of Ghaddar et al. [12] and compared well with the predictions of Gandhidasan correlations for the dehumidifier operation [13]. The dehumidifier model results of exit air temperature and humidity and liquid desiccant temperature and concentration were in excellent agreement with published correlations' predictions of Gandhidasan [13].

4.2. Dehumidification condenser coil

The modeling of cooling and dehumidification of the coil operation is adopted from the quasi-static model of Braun et al. [24] and modified by Zhou and Braun [25] to predict outlet air temperature and humidity conditions for known air inlet conditions leaving the solar still. Their model prediction of air and water outlet conditions is known to work very well under steady state operation. This model has been applied and tested in previous applications by the authors [26,27]. For modeling purposes the dehumidification condenser coil is divided into two zones: a dry and a wet zone. In the dry zone, the temperature of the air will drop assuming one dimensional heat transfer with the surrounding reservoir water according to the following equation:

$$\frac{\partial T_a}{\partial x} = -\frac{h_{ca}\pi D_i}{\dot{m}_a C_{pa}(T_a - T_{ti})} \tag{6}$$

where T_{ti} is the inner tube temperature and D_i is the inner coil diameter. The first term represents the convective energy change of air and the second term represents the heat exchange with the inner surface temperature of the tube. The inner surface temperature of the tube is related to the water temperature T_w in the reservoir by

$$h_c\pi D_i(T_a - T_{ti}) = \frac{(T_{ti} - T_W)}{R_{total}} \tag{7}$$

where R_{total} is the overall heat resistance between the inner tube surface and the water in the reservoir. The dry zone is restricted in the area starting from the entrance of the tube and ends in the location where the temperature of the passing air reaches its dew point temperature. The modeling of the remaining part of the dehumidification coil, wet zone, is adopted from the quasi-static model of Braun et al. [24] to predict outlet air temperature and humidity conditions for known air inlet conditions entering the coil. In the wet zone, the air undergoes both a sensible and latent heat transfer given by

$$C_{pa}\frac{\partial T_a}{\partial x} + h_{fg}\frac{\partial W_a}{\partial x} + \frac{h_{c,a}\pi D_i}{\dot{m}_a}(T_a - T_{ti}) + \frac{h_m\pi D_i}{\dot{m}_a}h_{fg}(W_a - W_{sT}) = 0 \tag{8}$$

where W_{sT} is the saturation humidity ratio at the inner tube surface temperature. To solve the above equations, it requires the coil geometric parameters, conditions of the air at the inlet of the coil and the reservoir sink temperature (available sea water) that depend on depth from which it is extracted. Note that the above model is a steady state model that will be used to simulate the quasi-steady operation of the humid air leaving the regenerator.

4.3. Parabolic solar concentrator

The rate of regeneration heat needed to attain a regeneration temperature of T_{reg} is given by

$$Q_R = \dot{m}_l(C_{pw} + Y_{lod}C_{pw})(T_{reg} - T_{lohe}) \quad (9)$$

where $\dot{m}_l$ is the flow rate of $CaCl_2$, T_{lohe} is the liquid desiccant temperature at outlet of heat exchanger and entering the solar heater, °C, and Y_{lod} is the moisture content at outlet of the dehumidifier. The solar collector system is composed of several modules of widely spread standard parabolic collector type that collects and stores solar energy in a water storage tank. Each module is 2.4 m long with diameter of 1.2 m. The transient performance of the collector-tank system is simulated numerically using the theory of Hottel and Whillier presented by Duffie and Beckman [28]. The useful heat gain of water in the collector is obtained by applying an energy balance that indicates the distribution of incident solar energy into useful heat gain, thermal losses and optical losses with a time step between 0.0833 up to 0.15 h depending on system flow rate. An expression for the useful heat gain is given by

$$Q_u = F_R A_a \left[S - \frac{A_r}{A_a} U_L (T_i - T_a) \right] \quad (10)$$

where T_i is the inlet water temperature to the collector, T_a is the ambient air temperature, U_L is the overall heat transfer loss coefficient and F_R is the heat removal factor. An energy balance on the associated well-mixed storage tank in which the concentrator circuit coil is embedded gives

$$(\rho C_{pw} V)_s \frac{dT_s}{dt} = \bar{Q}_u - L_s - (UA)_t (T_s - T_a) \quad (11)$$

where T_s is the well mixed tank fluid temperature, $\bar{Q}_u$ is the effective useful heat gain corrected for embedded coil effectiveness, L_s is the extracted load from the tank by liquid desiccant flow before entering the regenerator from the solar system, V_s is the tank volume. The liquid desiccant temperature at outlet of the solar concentrator system $T_{lo,sh}$ is given by

$$T_{lo,sh} = T_{li,sh} + eff_{sh}(T_s - T_{li,sh}) \quad (12)$$

where $T_{li,sh}$ is the temperature at inlet to the solar heater and eff_{sh} is the effectiveness of the solar heater (=0.9).

4.4. Integrated LDS model solution

To build the simulation model for the operation of the combined solar-powered *LDS*, it is important to integrate the various system component and process models to ensure that the regeneration process is totally powered by solar energy. The simulation model of the liquid desiccant dehumidifier and regenerator predicts the exit air and liquid desiccant temperature and humidity, the parabolic solar concentrator and storage tank model predicts the exit liquid desiccant temperature for known desiccant flow rate, the cooling coil simulation model predicts the exit conditions of air from the coil and the amount of condensate all subject to time-varying solar and ambient temperature and humidity.

The temporal calculations of the solar collector-tank system proceeds using first order Euler-Forward integration scheme at an initial temperature of the storage tank and inlet water temperature to the collectors equal to the ambient temperature for the given day at the start of the operation. The hourly values of direct solar radiation incident on the collectors and the values of ambient temperatures, wind speed and direction are derived directly from actual hourly measured weather data files of Beirut and are used directly in the simulation program. In the transient analysis, the ambient conditions are not constant but they are taken from the hourly-measured values for the typical day of the month [29]. The simulations are performed on the *LDS* module for Beirut weather using a time step of 1 min where every 60 min are averaged into an hourly value. Closing the iteration loop, the moisture content of the desiccant exiting the regenerator should match the moisture content of the desiccant at inlet of the dehumidifier. The system is assumed to behave in a quasi-steady-state manner; i.e. the variables, while varying from hour to hour, are considered constant during every hour of analysis and the unsteady terms in the governing equations are neglected. The numerical model calculates the following parameters at various bed heights and inlet conditions of the liquid desiccant and air and solution flow rates: air and liquid desiccant temperatures, air humidity ratios, liquid desiccant moisture content in the packed beds, amount of produced water, and temperature of the water in the storage tank.

5. Case study

A case study of a typical residential space (80 m^2) in line with the practice of 40 W/m^2 maximum cooling is considered for assessing the feasibility of the solar-powered calcium chloride *LDS* in providing thermal comfort over the 9 h of operation and produce 15 l of fresh water over that period during the summer months of Beirut climate. The building envelop have conductance values of glass = 3.4 W/m^2 K, an overall wall conductance, U = 1.3 W/m^2 K, and roof conductance = 0.6 W/m^2 K. The window to wall ratio is 20% and the sensible heat factor is taken as 0.8. Fig. 3 shows the hourly air conditioning load profile of the house for the months of June and August for design room values of relative humidity

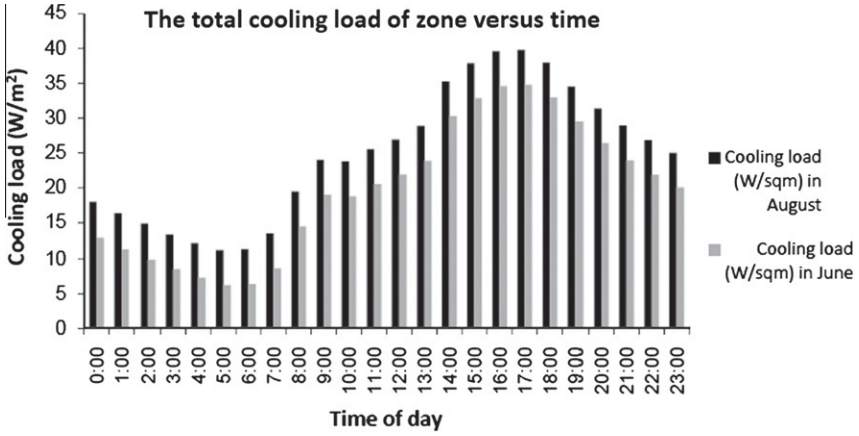

Fig. 3. The hourly cooling load for the months of June and August.

RH = 50% and room temperature of 25 °C. As mentioned earlier, the critical need to be met is cooling in August (high temperature and humidity ambient air) while the most critical need to be met in June is the fresh water since the air is relatively drier and at lower temperature. Upon sizing the major components of the *LDS* which include the dehumidifier/regenerator, cooling coil, heat exchangers, and solar concentrators, the optimum operation of the *LDS* is investigated. The three variables of the hybrid circuit include, the air flow rate going into our dehumidifier, the desiccant flow rate, and the number of solar concentrators. From the system simulation, the conditions for both humidity ratio and temperature leaving the dehumidifier are found. The dry air leaving the dehumidifier is treated by entering into a sensible heat exchanger to cool the air supplied to the space. We can find the space load such that the comfort level of occupant is attained by setting the predicted mean vote (PMV) to 0.5 [30]. At the peak load of 40 W/m^2, the required supply air mass flow rate is 1.0 kg/s. The desired hourly supply air flow rate and conditions can be found over the hours of operation of the system. In addition, comfort level for the occupant is assessed and the minimum circulation air motion within the space is found to achieve the desired level of PMV at 0.5.

Once the supply air flow rate into the space is known, the corresponding liquid desiccant flow rate is found using the best ratio practice ratio of 2.54 of desiccant to air flow rate [11]. To verify that this is the best ratio for use in our work, we plot in Fig. 4 the variation of the predicted collected water over 9 h of operation versus the liquid desiccant to air flow rate ratio of the designed system using six solar concentrators and 1 kg/s of air flow for the month of August. It is clear that the best operating ratio for the system is indeed around r = 2.5. The number of concentrators is dependent on the regeneration temperature. The number of needed solar concentrators will be associated with the minimum regeneration temperature of 50 °C which will be considered the reference design base case for producing the 15 l of fresh water and meeting the air conditioning needs at a heat sink temperature of 20 °C. The *LDS* simulations are run at air flow rate of 1 kg/s for the months of June, July, August and September based on loads of each month and their weather data. It was found that for the month of June with lowest ambient humidity the amount of water produced is less than the set requirement of 15 l. A 1.205 kg/s is required of air mass flow rate through the *LDS* towers to produce the 15 l of water for the month of June. Table 1 presents the *LDS* base case design parameters of the liquid desiccant dehumidifier/regenerator module and the parabolic solar concentrator module. The solar concentrators' circulation fluid is fed into an insulated storage tank volume 400 l with a heat exchanger effectiveness of 0.9 to heat the liquid desiccant entering the regenerator (see Fig. 1). The *LDS* base case operation assumes a heat exchanger effectiveness of 0.7 and a heat sink of 20 °C [11].

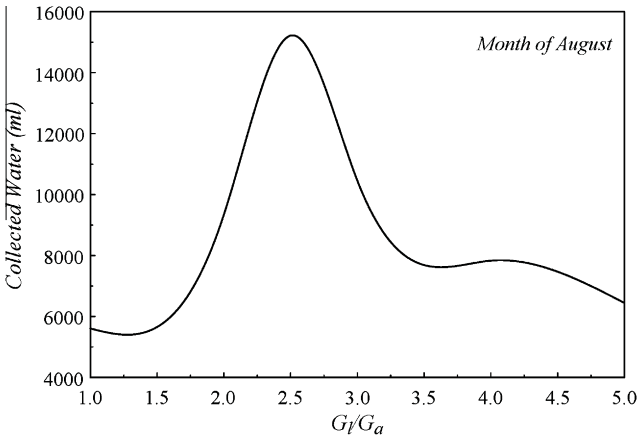

Fig. 4. The variation of the predicted collected water versus the liquid desiccant to air flow rate ratio of the designed system using six solar concentrators and 1 kg/s of air flow for the month of August.

Table 1
The *LDS* base case design parameters of the liquid desiccant dehumidifier/regenerator module and the parabolic solar concentrator module.

Design parameter	Value
Liquid desiccant dehumidifier/regenerator towers	
Air flow rate	1 kg/s
Desiccant flow rate	2.5 kg/s
Ratio of air flow rate of dehumidifier/regenerator	1
Height	1.5 m
Length	1 m
Regeneration temperature	50 °C
Temperature of desiccant into dehumidifier	30 °C
Parabolic solar concentrator module	
Length of solar concentrator	2.4 m
Width of solar concentrator	1.2 m
Absorbed solar radiation per area aperture	600 W/m^2
Receiver emittance	0.31
Absorber diameter	0.06 m
Transparent envelope outer diameter	0.09 m
Thickness of transparent envelope	0.004 m
Heat transfer of tube	300 W/m^2 °C
Loss coefficient	3.82 W/m^2 °C
Thermal conductivity of tube	16 W/m °C
Wall thickness of tube	0.05 m
Flow rate of water or fluid in collector	0.0537 kg/s
Specific heat of fluid passing collector (i.e. water)	4186 J/kg °C
Temperature of collector	100 °C

Table 2
The hourly and total amount of condensed water for the two extreme air flow rates of 1 kg/s and 1.205 kg/s over the cooling season.

Air flow rate = 1 kg/s Produced water (ml/h)					Air flow rate = 1.205 kg/s Produced water (ml/h)			
Time of day	June	July	August	September	June	July	August	September
9:00 AM	287	503	514.8	385	423	731	770	499
10:00 AM	676	875	889.2	700	810	1376	1420	883
11:00 AM	1177	1316	1461	1190	1120	1772	1827	1160
12:00 PM	1280	1784	1836	1200	1824	2233	2298	1871
1:00 PM	1250	1909	1955	1480	1870	2501	2553	1916
2:00 PM	1303	2289	2334	1680	2037	2752	2797	2130
3:00 PM	990	1791	1861	1010	2003	2330	2442	2056
4:00 PM	800	1510	1534	890	1810	1821	1896	1830
5:00 PM	680	1528	1534	789	1705	1843	1873	1728
6:00 PM	590	1505	1510	710	1503	1822	1866	1527
Total (ml/day)	9033	15,010	15,434	10,034	15,111	19181	19742	15,606

Simulations are performed for different heat sink temperatures ranging from 16 to 20 °C for cooling the liquid desiccant entering the dehumidifier. The lower the temperature of the heat sink the more potential exists to desiccant absorption of water leading to more transfer of moisture to the air in the regenerator. This in turn means that lower supply air mass flow rate is needed to produce the same amount of water; nevertheless this will lead to the use of more solar concentrator modules for heating the desiccant. The *LCC* cost will determine the optimal heat regeneration temperature and its associated air flow rate for heat sink temperature above the base case value.

6. Results and discussion

The *LDS* hourly operational performance data will be presented for the month of August for the base simulation case of heat sink temperature of 20 °C. Then, the cooling season energy consumption will be presented for the solar-powered *LDS* over the cooling demand months of June, July, August, and September while collecting the 15 l of fresh water over 9 h of operation. This will then be followed by presentation of optimized design parameters at different heat sink temperatures.

According to the design calculations for insuring the daily delivery of 15 l during the summer season, six concentrator modules are needed as determined by the operation of the system in the month of June (the summer month of the least solar radiation) in Beirut humid weather. The air flow rate needed for air conditioning in June is 1.18 kg/s, which is not enough for water production. So in order to meet both air conditioning and water production needs, we increase our flow rate to 1.205 kg/s to achieve both needs in June. The corresponding desiccant flow rate at the selected $r = 2.5$ ratio dictates the need for six solar concentrator modules to reach the required regeneration temperature. For the month of August the required air flow rate for production of the 15 l of fresh water is 0.97 kg/s while the dry air flow for air conditioning needs is 1.0 kg/s. Therefore, in order to meet both requirements of water and cooling in the month of August, the desiccant flow is 2.5 kg/s and six solar concentrator modules are needed. Table 2 presents the hourly amount of condensed water for the two extreme air flow rates of 1.0 kg/s and 1.205 kg/s over the cooling season. It is clear that the water production requirement is controlled by the air flow rate that can be set differently for each month.

Simulation results for a typical day in August at 1 kg/s air flow at desiccant to air flow ratio of 2.54 are presented. Table 3 shows the air humidity ratio and temperature leaving the dehumidifier and regenerator for the base case of air flow rate of 1 kg/s at inlet liquid desiccant temperature of 30 °C and sink temperature of 20 °C. Fig. 5 shows the transient temperature in the storage tank and the incident solar radiation over a three day period taking into consideration the incident solar radiation on an hourly basis. It should be noted that the steady periodic values of the third day of simulation has been used in the calculation since we assume continuous operation of the system during the month of August using the reference day of August 15. The storage tank heat up between 7:00 AM and 9:00 AM in order to allow the temperature in the storage tank to increase to the desired 50 °C.

The dry air stream exiting the dehumidifier is sensibly cooled further using sea water source as available cooling source that varies between 16 °C and 20 °C depending on seawater withdrawal depth. The cooled dry air is used as supply air to the space. The hourly supply flow rate and supply air temperature to the space is then determined to meet the room air conditioning load. In addition, the minimum circulation air velocity in the space using a

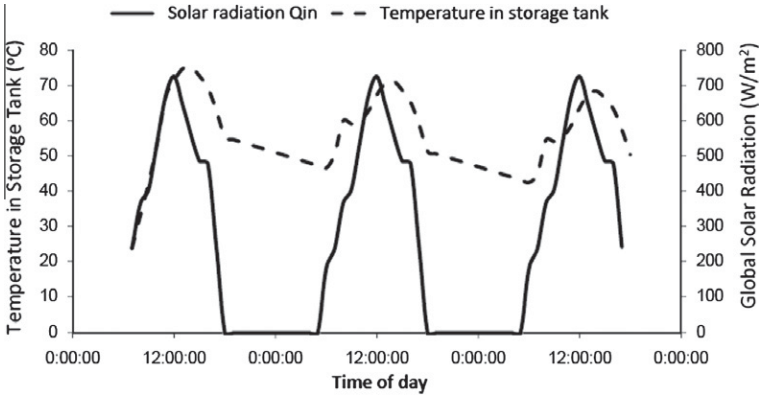

Fig. 5. The storage tank temperature and incident global solar radiation for typical August day in Beirut climate.

Table 3
The temperature and humidity ratios of air entering leaving dehumidifier during August for the base case of air flow rate of 1 kg/s at inlet liquid desiccant temperature of 30 °C and sink temperature of 20 °C.

Time	Ambient temp. (°C)	Ambient humidity ratio (kg H_2O/kg air)	Temperature exiting dehumidifier (°C)	Humidity ratio leaving dehumidifier (kg H_2O/kg air)	Global solar radiation (W/m^2)	Temperature exiting Regenerator (°C)	Air humidity exiting regenerator (kg H_2O/kg air)
9:00 AM	25.1	0.017	26.1	0.0135	485.6	30.2	0.021
10:00 AM	26.3	0.018	27.2	0.014	560.7	29.5	0.022
11:00 AM	27.8	0.019	28.5	0.0145	646.1	31	0.023
12:00 PM	29.1	0.021	29.5	0.016	726.2	32.5	0.025
1:00 PM	30.1	0.021	30.0	0.016	671.0	33.3	0.025
2:00 PM	30.8	0.022	30.4	0.017	541.5	32.8	0.026
3:00 PM	31.0	0.021	30.5	0.016	406.6	33.8	0.025
4:00 PM	30.8	0.02	30.5	0.0155	364.8	33.4	0.024
5:00 PM	30.2	0.02	30.0	0.0155	236.6	32.7	0.024
6:00 PM	29.3	0.019	29.6	0.015	180.4	32.9	0.023

Table 4
The indoor humidity, temperature, and thermal comfort velocity needed in the space for the LDS system operated in August.

Time	Temperature of air exiting dehumidifier (°C)	Supply air temp (°C)	Space cooling load (W)	Supply air flow rate (kg/s)	Room temperature (°C)	Room humidity ratio (kg H_2O/kg air)	Required air circulation velocity in the space (m/s)
9:00 AM	26.1	20.2	1920.4	0.637	23.9	0.015	1
10:00 AM	27.2	20.7	1900.3	0.63	24.6	0.0155	1.3
11:00 AM	28.5	21	2041.0	0.677	25.9	0.016	1.37
12:00 PM	29.5	22	2151.5	0.714	26.9	0.0173	1.44
1:00 PM	30.0	22.5	2309.9	0.766	27.4	0.0175	1.47
2:00 PM	30.4	22.9	2820.9	0.935	27.9	0.0173	1.5
3:00 PM	30.5	23	3028.3	1.00	28	0.017	1.5
4:00 PM	30.5	23	3165.0	1.05	28.1	0.0165	1.49
5:00 PM	30.0	22.5	3180.8	1.05	27.3	0.0165	1.43
6:00 PM	29.6	22.1	3035.9	1.00	26.1	0.0155	1.4

ceiling/wall fan is calculated such that *PMV* in the space is equal to 0.5 to ensure attainment of thermal comfort [14–16]. Table 4 presents the month of August data on supply air flow rate, temperature and relative humidity in addition to the attained room conditions and minimum room air circulation velocity to attain a *PMV* of 0.5 [31]. It is clear that comfort conditions can be met without need to use conventional system.

To provide optimal design by calculating the life cycle cost that corresponds to changes in the design heat sink temperature, simulations of the *LDS* operation are repeated for all the cooling month. The system life is assumed 20 years and the interest rate is taken as 3%. If the sink temperature is decreased to 16 °C, a potential increase in regeneration temperature up to 55 °C is expected compared to 50 °C when the sink temperature is 20 °C. The advantage of lower sink temperature is that it permits decreasing the required *LDS* air flow rate to 0.8 kg/s compared to 1.205 kg/s for the months of June and September. For the months of July and August, this decrease in flow rate is not possible since the air conditioning load is the governing factor and the conditions of air leaving the dehumidifier are not affected. In general, a lower air flow rate reduces the operation cost but increases the regeneration temperature. Higher regeneration temperature increases the initial capital cost since it requires installation of more solar concentrator modules. The case of the design at heat sink temperature of 20 °C represents the design with the minimum number of concentrator modules (lowest initial cost). The results are presented for the investment life cycle cost (*LCC*) defined in Eq. (14) to find the optimal regeneration temperature that justifies the investment in adding solar concentrator modules. The life cycle cost is calculated as the payback period as the ratio of the invested capital over saved $ in operation cost. The cost of the parabolic solar concentrator module is assumed 1000 $/module taken from standard unit prices available in current market and the electrical energy cost is assumed 0.12 $/kW h.

Table 5
Operational data at four heat sink temperature at different re-generation temperatures and the required air flow rate.

Sink temperature (°C)	Regeneration temp. (°C)	Air flow (June) kg/s	Air flow (August) kg/s	Air flow rate required (kg/s)
16 °C	50	0.88	1.01	1.01
	51	0.87	1.00	1.00
	52	0.85	0.98	0.98
	53	0.83	0.97	0.97
	54	0.82	0.96	0.96
	55	0.8	0.95	0.95
17 °C	50	0.97	1.02	1.02
	51	0.95	1.00	1.00
	52	0.93	0.99	0.99
	53	0.91	0.98	0.98
	54	0.90	0.97	0.97
18 °C	50	1.10	1.05	1.1
	51	1.08	1.02	1.08
	52	1.06	1.00	1.00
	53	1.05	0.99	1.05
19 °C	50	1.135	1.045	1.135
	51	1.12	1.03	1.12
	52	1.105	1.02	1.105

For a heat sink temperature of 17 °C, it is found that the design number of solar concentrator modules changes from 6 modules to 7 modules when regeneration temperature is changed 50–54 °C with an optimal operating regeneration temperature at 51.7 °C. Table 5 provides operational data at four heat sink temperature at different re-generation temperatures and the corresponding air flow rate. Fig. 6 shows the life cycle cost in years versus the regeneration temperature for different heat sink temperatures. It is clear that the optimal regeneration temperature increases with decreased heat sink temperature with values of 50 °C, 50.8 °C, and 52 °C corresponding to sink temperatures of 20 °C, 18 °C, and 16 °C.

If we compare water production cost to typical conventional water making machines which use a vapor compression cycle for home application produces for a cost of 0.084 $/l, we find that the cost for the *LDS* to produce this same amount of water is less at 0.0675 $/l averaged over all the months at 0.12 $/kW h. The extracted water might by expensive, but it is an alternative for small scale applications extracting water from the atmosphere. New commercial water production machines from air amounts cost

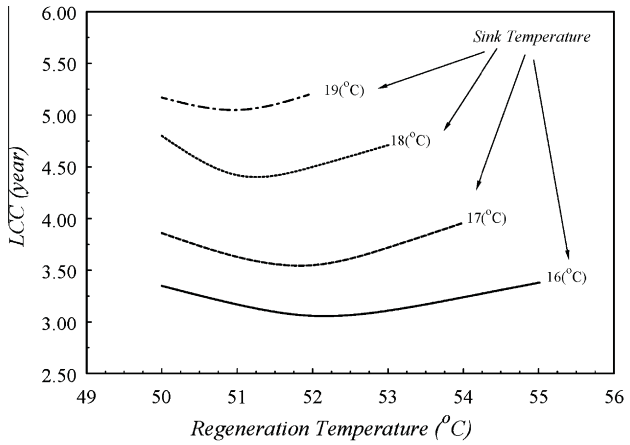

Fig. 6. The *LCC* as a function of regeneration temperature at different heat sink temperatures.

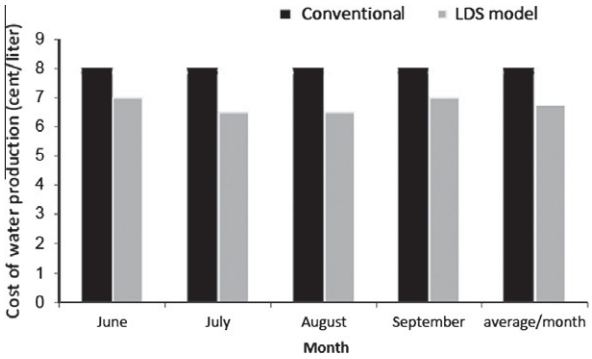

Fig. 7. The cost of water production in cent/liter for each of the cooling months from the *LDS* and conventional vapor compression commercial system.

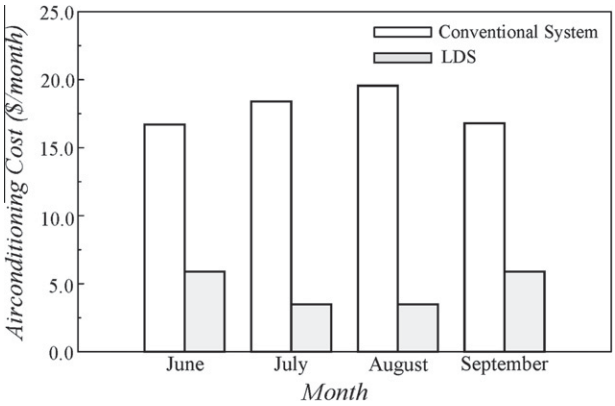

Fig. 8. The monthly cost of both the conventional and current proposed *LDS*.

0.66 kW h/l [32]. The de-mineralized water obtained from the cooling water requires additives such as flavoring agents and minerals to make it potable. For each five gallons of water two tablespoons of mineral drops should be added [34]. The cost of these additives is usually small when considering large scale of de-mineralized water, however with small quantities in the range of 15 l the best option is to mix it with brackish water and disinfect the mixture by ozonolysis [34]. The consideration of water cost will only be presented in terms of energy use. Fig. 7 shows the average monthly cost of water production using the *LDS* and the commercial water production from the atmosphere. Note that the most expensive month is June due to its lower atmospheric humidity.

The air conditioning operational cost for the case study when using a vapor compression conventional system will be compared with the cost of the *LDS*. The cooling load and the sizing of the conventional system are obtained using Visual DOE 4.0 [33] to estimate the monthly electrical energy consumption. The input to the software were the geometric and envelop parameters of the case study with the same internal load and comfort level (see Fig. 3 of cooling load of the residence case study). For the conventional system we will use the optimal operation value for sink temperature of 17 °C to cool the temperature of condenser' air in a cross flow heat exchanger at efficiency of 0.85. The drop in the hourly ambient air temperature for cooling the condenser improves conventional system performance [35]. We used Motta and Domanski [35] chart of the coefficient of performance COP variation with ambient temperature (reference COP is 3.7 for ambient temperature of 32 °C) to correct the conventional system hourly COP and calculate the hourly energy consumption. The calculations are based on the corrected coefficient of performance of the conventional system operated for the same number of hours as the *LDS*. Fig. 8 shows the monthly cost of both the conventional and current proposed *LDS*. The month of August has the highest electrical energy consumption out of the cooling season for both systems, but the *LDS* operational cost is less one third of energy consumed by the conventional system. Over the life cycle of 20 years, the conventional system will require on average 341 $/month for electrical energy consumption compared to an average of 105.5 $/month. More savings are foreseen when we consider the dual function of the *LDS*.

7. Conclusions

It is demonstrated that it is feasible to use a solar-powered liquid desiccant system that meets both needs the production of fresh water and space environmental comfort at minimum cost. Using simulation models of the various components of the *LDS*, we have to optimally sized and set the system operational parameters to predict its performance in terms of water output and energy utilization in Beirut humid weather.

It is found in the case study that the heat sink temperature is a critical optimization parameter and dictates the appropriate regeneration temperature within the constraints of operation of the system to deliver its outputs of fresh water and dry cool air stream. A lower heat sink temperature at 17–18 °C with an additional solar collector would prove economically feasible while meet our set requirements compare to the base case sink temperature of 20 °C.

The importance of this proposed system is that it saves energy, produces water, creates comfortable built in environment using renewable energy source and without any harm to the environment since water extraction is from the atmosphere. Future work will explore the possibility of extending the *LDS* operation all year including the heating season and using the regenerator stream for heating the dry air for space heating. In addition, future work would address the effect of the type of the chemical desiccant on improving system performance even though calcium chloride is the safest desiccant to use. We can investigate whether the use of different chemicals with lower specific heat would be more economical in reducing regeneration energy needed even though the initial cost of such desiccants might be high.

Acknowledgments

The financial support of the Munib Masri Institute for Energy and Natural Resources, the ASHRAE Senior Project Award 2010-11, District Cooling PRO Engineering of UAE, and the Qatar Chair in Energy Studies Endowment Fund are all highly acknowledged.

References

[1] Al-Faifi H, Al-Omran AM, Nadeem M, El-Eter A, Khater HA, El-Maghraby SE. Soil deterioration as influenced by land disposal of reject brine from Salbukh water desalination plant at Riyadh, Saudi Arabia. Desalination 2010;250:479–84.
[2] Eicker U, Schneider U, Schumacher J, Ge T, Dai Y. Operational experiences with solar air collector driven desiccant cooling systems. Appl Energy 2010;87(12):3735–47.
[3] Zhai XQ, Wang RZ, Wu JY, Dai YJ, Ma Q. Design and performance of a solar-powered air-conditioning system in a green building. Appl Energy 2008;85(5):297–311.
[4] Chua KJ, Chou SK, Yang WM. Advances in heat pump systems: a review. Appl Energy 2010;87(12):3611–24.
[5] Praene JP, Marc O, Lucas F, Miranville F. Simulation and experimental investigation of solar absorption cooling system in Reunion Island. Appl Energy 2011;88(3):831–9.
[6] Sozen A, Ozalp M. Solar-driven ejector-absorption cooling system. Appl Energy 2004;80(1):97–113.
[7] Fumo N, Goswami DY. Study of an aqueous lithium chloride desiccant system: air dehumidification and desiccant regeneration. Sol Energy 2002;72(4):351–61.
[8] Afandizadeh S, Foumeny EA. Design of packed bed reactors: guide to catalyst shape, size, and loading selection. Appl Therm Eng 2001;21(6):669–82.
[9] Al-Farayedhi AA, Gandhidasan P, Younas AS. Regeneration of liquid desiccant using membrane technology. Energy Convers Manage 1999;40:1405–11.

[10] Al-Sulaiman FA, Gandhidasan P, Zubair SM. Liquid desiccant based two-stage evaporative cooling system using reverse osmosis (RO) process for regeneration. Appl Therm Eng 2007;27(15):2449–54.
[11] Elsarrag E. Evaporation rate of a novel tilted solar liquid desiccant regeneration system. Sol Energy 2008;82:663–8.
[12] Ghaddar N, Ghali K, Najm A. Use of desiccant dehumidification to improve energy utilization in air-conditioning systems in Beirut. Int J Energy Res 2003;27(15):1317–38.
[13] Gandhidasan P. A simplified model for air dehumidification with liquid desiccant. Sol Energy 2004;76:409–16.
[14] Messaoudene A, Imessad K, Belhamel M. Effect of ventilation on thermal comfort measured by DTS-application to a typical home in Algerian conditions. Renew Energy 2010;35:629–36.
[15] Liping W, Hien WN. The impact of ventilation strategies and facades on indoor thermal environment for naturally ventilated residential buildings in Singapore. Build Environ 2007;42:4006–40015.
[16] Arens E, Xu T, Miura K, Hui Z, Fountain M, Bauman F. A study of occupant cooling by personally controlled air movement. Energy Build 1998;27: 45–59.
[17] Narayan GP, Sharqawy MH, Summers EK, Lienhard JH, Zubair SM, Antar MA. The potential of solar-driven humidification–dehumidification desalination for small-scale decentralized water production. Renew Sust Energy Rev 2010;14:1187–201.
[18] Bourouni K, Chaibi MT, Tadrist L. Water desalination by humidification and dehumidification of air: state of the art. Desalination 2001;137:167–76.
[19] Parekh S, Farid MM, Selmana JR, Al-Hallaj S. Solar desalination with a humidification-dehumidification technique – a comprehensive technical review. Desalination 2004;160:167–86.
[20] Ettouney H. Design and analysis of humidification dehumidification desalination process. Desalination 2005;183:341–52.
[21] Xiong ZQ, Dai JY, Wang RZ. Development of a novel two-stage liquid desiccant dehumidification system assisted by $CaCl_2$ solution using exergy analysis method. Appl Energy 2010;87(5):1495–504.
[22] Radhwan AM, Gari HN, El-Sayed MM. Parametric study of a packed bed dehumidifier/regenerator using $CaCl_2$ liquid desiccant. Renew Energy 1993;3(1):49–60.
[23] Ertas A, Anderson EE, Kavasogullari E. Comparison of mass and heat transfer coefficients of liquid-desiccant mixtures in a packed column. J Energy Resour Technol 1991;113:1–6.
[24] Braun JE, Klein SA, Mitchell JW. Effectiveness models for cooling towers and cooling coils. ASHRAE Trans 1989;95(2):164–74.
[25] Zhou X, Braun JE. Simplified dynamic model for chilled-water cooling and dehumidifying coils-part 1: development (RP-1194). HVAC&R Res 2007;13(5):785–824.
[26] Mossolly M, Ghaddar N, Ghali K, Jensen L. Optimized operation of combined chilled ceiling displacement ventilation system using genetic algorithm. ASHRAE Trans 2008;143(2):541–54.
[27] Holman JP. Heat transfer. 8th ed. New York: McGraw-Hill; 1997. p. 488 [chapter 8].
[28] Duffie J, Beckman W. Solar engineering of thermal processes, 3rd ed. New York: Wiley; 2003 [chapter 7].
[29] Ghaddar N, Bsat A. Energy conservation of residential buildings in Beirut. Int J Energy Res 1998;32(2):523–46.
[30] Fanger BO. Thermal comfort analysis and applications in engineering. New York: McGraw Hill; 1982.
[31] ASHRAE. Handbook of fundamentals, American society of heating, refrigerating and air conditioning engineers. Atlanta, GA; 2005.
[32] Skywater®, 2009. <http://islandsky.com/products/home-and-office-water-making-machine>.
[33] Visual DOE 4.0 software. Architectural energy cooperation. San Francisco, USA; 2005 <http://www.archenergy.com>.
[34] Hafez A, El-Manharawyb S. Economics of seawater RO desalination in the Red Sea region, Egypt. Part 1: a case study. Desalination 2002;153:335–47.
[35] Motta SFY, Domanski PA. Performance of R-22 and its alternatives working at high outdoor temperatures. In: Proceedings of the eighth international refrigeration conference, July 25–28, 2000, West Lafayette, IN; 2000. p. 47–54.